research papers

Structure of β-trimyristin and β-tristearin from high-resolution X-ray powder diffraction data

Arjen van Langevelde, René Peschar* and Henk Schenk

Laboratory for Crystallography, Institute of Molecular Chemistry (IMC), Universiteit van Amsterdam, Nieuwe Achtergracht 166, 1018 WV Amsterdam, The Netherlands

Correspondence e-mail: rene@crys.chem.uva.nl

The crystal structures of β-1,2,3-tritetradecanoylglycerol (β-trimyristin or β-MMM) and β-1,2,3-trioctadecanoylglycerol (β-tristearin or β-SSS) have been determined from high-resolution synchrotron X-ray powder diffraction data. Grid search and Rietveld refinement have been used to determine and refine the structure, respectively. Both substances crystallize in space group $P\bar{1}$ with $Z = 2$. The unit-cell parameters for β-MMM are $a = 12.0626\,(6)$, $b = 41.714\,(1)$, $c = 5.4588\,(3)$ Å, $\alpha = 73.388\,(4)$, $\beta = 100.408\,(5)$ and $\gamma = 118.274\,(4)^{\circ}$. For β-SSS the unit-cell parameters are $a = 12.0053\,(7)$, $b = 51.902\,(2)$, $c = 5.4450\,(3)$ Å, $\alpha = 73.752\,(5)$, $\beta = 100.256\,(6)$ and $\gamma = 117.691\,(5)^{\circ}$. Soft-distance restraints have been applied to the molecules during refinement. For β-MMM the final R_p value obtained is 0.053 and for β-SSS the final R_p value is 0.041.

1. Introduction

Triacylglycerols (TAGs) and their mixtures, oils and fats, are applied in a wide range of consumer and health products. Owing to their polymorphic behaviour as a function of temperature the crystallization process is a key step in producing quality products. Since each TAG polymorph (γ, α, β' and β) has its own characteristic physical properties, the crystallized polymorph largely determines the physical properties of the final product. Therefore, this important class of compound has been the subject of thorough research for many years and their polymorphic crystallization behaviour one of the major topics therein.

To understand crystallization and polymorphic transformation processes crystal-structure information of the various polymorphs is indispensable. However, crystal-structure information of TAGs is very scarce and especially for the metastable polymorphs. So far five crystal structures of TAGs have been published, all crystallized in the β polymorph with a parallel zigzag-plane chain packing. Three structures from the β-stable $C_nC_nC_n$-type (n = even) series have been determined and on the basis of this a predictive model for the other series members has been built (Gibon *et al.*, 1984; Jensen & Mabis, 1963, 1966; Larsson, 1965; Van Langevelde *et al.*, 1999*a*). Other crystal structures of related TAG's in the β-phase are 2-(11-bromoundecanoyl)-1,1′-dicaprin ($CL^{Br}C$; Doyne & Gordon, 1968), being a bromine-containing analogue of the β'-stable $C_nC_{n+2}C_n$-type (n = even) series, the 1,2-dipalmitoyl-3-acetyl-*sn*-glycerol PP2 (Goto *et al.*, 1992) having one short acyl chain and the *trans* unsaturated 1,2,3-tri(*trans*-9-octadecenoyl)-

glycerol (trielaidin or EEE; Culot *et al.*, 2000). Crystal structures of TAGs in the β' polymorph are hardly available. A packing model and a crystal structure model at the atomic level for the β'-stable $C_nC_{n+2}C_n$-type (n = even) series have been proposed (Van Langevelde *et al.*, 1999*b*; Van de Streek *et al.*, 1999, respectively), but only recently for two members of this series a successful crystal structure determination and refinement has been carried out (Van Langevelde *et al.*, 2000).

This lack of TAG crystal structures is understandable because for successful structure determination of TAGs several major problems have to be solved. Starting with high-purity material a good-quality single crystal has to be grown, which demands perfectly controlled circumstances. In most cases, single crystals of TAGs are needle- or plate-shaped and tend to form twins. Having performed a good data collection, the data has to be indexed and integrated. Since the unit cells of TAGs have one large and one very short cell axis, most indexing programs fail to do the job, because they are optimized to index small molecules with three axes of small to moderate size or proteins with three large axes. Also integration is not straightforward, because some subcell-related reflections have a very high intensity while all others have moderate or weak intensity. This large ratio in intensity also directs the structure-solving process. As structural information about the hydrocarbon chain packing is dominantly present in the data set, the atomic coordinates of the glycerol moiety are hard to determine.

To overcome most of these problems, information provided by the homology between the members of TAGs series can be used. Since the molecules of a homologous series differ in chain length only, they are expected to have similar cells and crystal packing. For a triclinic crystal system cell axis and acyl chains can be parallelized by unit-cell transformation. Then, with the longest cell axis parallel to the acyl chains, the longest cell axis increases linearly with acyl chain lengthening, while the other cell parameters remain constant. After having successfully indexed the X-ray diffraction pattern for one member of a series, this relation between cell parameters and chain length can be used to predict and determine the cell parameters for other series members. Furthermore, knowing the crystal structure of one member of a homologous series, the crystal structure of the others can be predicted and determined more easily. In this way, on the basis of one single-crystal structure determination, the structure of other members of a TAG series can be determined from high-resolution X-ray powder diffraction (XRPD) data. Consequently, no exhausting efforts have to be undertaken to grow measurable single crystals for all series members. Obviously, this method is only applicable as long as the molecules of the series adopt identical crystal packing. In this paper the structures of β-1,2,3-tritetradecanoylglycerol (β-trimyristin or β-MMM) and β-1,2,3-trioctadecanoylglycerol (β-tristearin or β-SSS) are presented. Both are members of the β-stable $C_nC_nC_n$-type (n = even) TAG series for which the above-mentioned predictive model was built and for which only unit-cell parameters were available (β-MMM in Van Langevelde *et al.*, 1999*a*; β-SSS in Skoda *et al.*, 1967; De Jong & Van Soest,

1978). The structures of β-MMM and β-SSS were determined from high-resolution synchrotron XRPD data, illustrating the appropriate use of the β-$C_nC_nC_n$-type (n = even) series' homology.

2. Materials and methods

2.1. Samples, sample preparation and data collection

β-MMM and β-SSS were purchased as whitish crystalline powders from Sigma Chemical Co. (St Louis, USA) with a purity of ~99%. XRPD photographs of MMM and SSS were made using an Enraf–Nonius FR 552 Guinier Johansson camera (Enraf–Nonius, Delft, The Netherlands) equipped with a Johansson monochromator (Roberts & Parrish, 1962) using Cu $K\alpha_1$ radiation, λ = 1.54060 Å. The samples were prepared by pressing the powder to a thin layer onto Mylar foil. To improve particle statistics the sample holder was rotated in the specimen plane during exposure. For indexing the patterns the accurate positions of 74 lines for MMM and 33 lines for SSS were collected by reading out the Guinier photographs with an optical instrument.

A high-resolution synchrotron XRPD pattern of MMM was made at beamline BM01 of the Swiss–Norwegian CRG at the European Synchrotron Radiation Facility (ESRF, Grenoble, France) with a fixed wavelength of 0.99542 Å. For data collection a capillary with a diameter of 1.5 mm was filled with powder and rotated during exposure. Continuous scans were made at room temperature from 2.0 to 15.0° 2θ with 0.3° 2θ min^{-1} and from 15.0 to 60.0° 2θ with 0.1° 2θ min^{-1}. After data collection the scans were binned at 0.005° 2θ. A second high-resolution synchrotron XRPD pattern of MMM was made (BM16; ESRF, Grenoble, France; Fitch, 1996) with a fixed wavelength of 0.699716 Å. For data collection a capillary with a diameter of 1.5 mm was filled with powder and rotated during exposure. Continuous scans were made at room temperature from 0.0 to 52.0° 2θ with 0.5° 2θ min^{-1} and a sampling time of 50 ms. After data collection the scans were binned at 0.005° 2θ.

An XRPD pattern of SSS was made at the high-resolution X-ray powder diffractometer (BM16; Fitch, 1996) at ESRF (Grenoble, France) with a fixed wavelength of 0.650515 (1) Å. For data collection a capillary with a diameter of 1.5 mm was filled with powder and rotated during exposure. Continuous scans were made at room temperature from 0.0 to 30.0° 2θ with 0.5° 2θ min^{-1} and a sampling time of 50 ms. After data collection the scans were binned at 0.004° 2θ.

2.2. Structure determination, refinement and comparison

The lines obtained from the Guinier powder-diffraction photographs of MMM and SSS were indexed using the program *ITO* (Visser, 1969) and manual interference. The resulting unit-cell parameters were refined on their synchrotron data using the program *UnitCell* (Holland & Redfern, 1997). In order to obtain accurate reflection intensities a full-pattern decomposition (FPD) was started: the synchrotron XRPD pattern was fitted employing a split-type pseudo-Voigt

research papers

Table 1
Unit-cell parameters for β-MMM.

Predicted values from overlap-model unit-cell setting (Van Langevelde *et al.*, 1999*a*); initially determined values: transformation matrix used to transform this unit cell in the refined one; refined values conform to the overlap-model unit-cell setting.

Cell parameter	Predicted	Initially determined	Refined
a (Å)	12.07	12.063 (6)	12.0626 (6)
b (Å)	41.72	41.369 (3)	41.714 (1)
c (Å)	5.47	5.4597 (4)	5.4588 (3)
α (°)	73.6	74.588 (5)	73.388 (4)
β (°)	100.5	100.409 (5)	100.408 (5)
γ (°)	118.7	117.944 (4)	118.274 (4)
V (Å^3)	2314.2	2315.4 (2)	2314.7 (2)

Transformation matrix
$$\begin{pmatrix} \bar{1} & 0 & 0 \\ 3 & 1 & \bar{3} \\ 0 & 0 & 1 \end{pmatrix}$$

Table 2
Refined preferred-orientation parameters of β-MMM and β-SSS.

ijp	C_{ijp} β-MMM	β-SSS
20+	0.248	0.181
21+	0.245	0.045
21−	−0.194	−0.124
22+	0.146	0.051
22−	−0.195	0.129
40+	−0.012	0.372
41+	−0.141	−0.136
41−	0.032	−0.097
42+	−0.092	−0.124
42−	0.059	0.076
43+	−0.123	0.260
43−	−0.138	−0.057
44+	−0.156	−0.252
44−	0.021	0.069

peak-profile function (Toraya, 1986) and decomposed using the program *MRIA* (Zlokazov & Chernyshev, 1992). A starting model for β-MMM and β-SSS was made originating from the crystal structure of β-1,2,3-trihexadecanoylglycerol (β-tripalmitin or β-PPP; Van Langevelde *et al.*, 1999*a*) using the program *Cerius*^{2} (Molecular Simulations Inc., 1995). For β-MMM the $-CH_2-CH_3$ moiety at the end of each palmitic chain was replaced by an H atom. For β-SSS the required chain length and chain orientation was obtained by replacing one H atom at the end of each palmitic chain by a $-CH_2-CH_3$ moiety and by setting the dihedral angles of these hydrocarbon chain ends to the staggered conformation. The geometry of these chain ends was optimized by energy minimization using the Universal Force Field (Rappé *et al.*, 1992). To position the possible models of β-MMM and β-SSS in their asymmetric unit, grid-search procedures (Chernyshev & Schenk, 1998) were applied to 200 low-order reflections obtained by decomposition of the synchrotron XRPD patterns. The obtained translational and rotational parameters were refined, followed by a full-pattern Rietveld refinement (RR). During refinement soft restraints were applied to the atomic distances (σ is ~1% of the ideal bond lengths). Under these restrictions the coordinates of all O and C atoms as well as isotropic atomic displacement parameters (U_{iso}) were refined for both β-MMM and β-SSS. The U_{iso} values of all C atoms were coupled as well as the U_{iso} values for all O atoms. The positions of the H atoms were calculated at 0.95 Å from
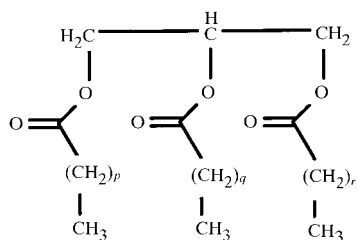
their carrier and the U_{iso} values were fixed at 0.05 Å^2. Preferred orientation was refined using the first 14 parameters of the symmetrized harmonics-expansion method (Ahtee *et al.*, 1989; Järvinen, 1993) for both MMM and SSS.

In order to compare their structural correspondence, the crystal structures of β-MMM, β-SSS and β-PPP were matched by minimizing the distance between corresponding C and O atoms, resulting in an overall r.m.s. (root mean square) value expressing the quality of the fit.

3. Results and discussion

The chemical structure diagram of MMM and SSS is shown in Fig. 1. Unit-cell parameters for β-MMM are listed in Table 1. With two $C_{45}H_{86}O_6$ molecules per unit cell the calculated density is 1.04 g cm^{-3}. Like the space group of the known β-$C_nC_nC_n$-type (n = even) TAGs, the space group of β-MMM is $P\bar{1}$. The FPD applied to the 2.0–40.0° 2θ region of the synchrotron pattern (measured at BM01) resulted in an R_p value of 0.082, an R_{wp} value of 0.114 and a χ^2 of 4.1. The RR applied to a 2θ range (of the diagram measured at BM16) of 1.495–30.005° resulted in a final fit between the calculated and experimental XRPD pattern with an R_p value of 0.053, an R_{wp} value of 0.070, an R_{Bragg} value of 0.102 and χ^2 of 3.9 (Fig. 2). Without correction for preferred orientation the R_p value was 0.082, the R_{wp} value 0.113, the R_{Bragg} value 0.158 and χ^2 was 6.3. The refined parameters for preferred orientation are listed in Table 2. The conformation of the β-MMM molecule in the refined crystal structure is shown in Fig. 3, the fractional atomic coordinates have been deposited[1] and the value ranges of selected geometric parameters are listed in Table 3.

Unit-cell parameters for β-SSS are listed in Table 4. Also for β-SSS the space group is $P\bar{1}$ and with one $C_{57}H_{110}O_6$ molecule in the asymmetric unit the calculated density is 1.03 g cm^{-3}. The FPD applied to the 1.0–20.0° 2θ region of the synchrotron

Figure 1
Chemical structure diagram of a triacylglycerol. For MMM $p = q = r = 12$ and in the case of SSS $p = q = r = 16$.

[1] Supplementary data for this paper are available from the IUCr electronic archives (Reference: NA0112). Services for accessing these data are described at the back of the journal.

Table 3
Value ranges for selected geometric parameters (Å^2, °) in the case of β-MMM.

C=O	1.25–1.27
C—O	1.30–1.47
C—C	1.46–1.59
O—C—C	115–119
O=C—C	121–125
O=C—O	119–124
C—O—C	116–122
C—C—C	109–115

Table 5
Value ranges for selected geometric parameters (Å^2, °) in the case of β-SSS.

C=O	1.24–1.28
C—O	1.24–1.47
C—C	1.48–1.59
O—C—C	112–118
O=C—C	122–128
O=C—O	119–126
C—O—C	111–123
C—C—C	108–116

Table 4
Unit-cell parameters for β-SSS.

Refined values from Langevelde *et al.*, 1999*a*); predicted values from the overlap model; third column, literature values after transformation from Skoda *et al.* (1967); fourth column, literature values after transformation from De Jong & Van Soest (1978).

Cell parameter	Refined	Predicted	Literature	Literature
a (Å)	12.0053 (7)	12.07	11.97	12.11
b (Å)	51.902 (2)	51.95	52.08	53.83
c (Å)	5.4450 (3)	5.47	5.45	5.45
α (°)	73.752 (5)	73.6	72.8	73.1
β (°)	100.256 (6)	100.5	101.0	100.2
γ (°)	117.691 (5)	118.7	117.9	121.3
V (Å^3)	2879.6 (2)	2881.7	2862.7	2902.1
			$\bar{1}$ 0 0	1 1 0
Transformation matrix			1 $\bar{2}$ $\bar{1}$	$\bar{4}$ 1 $\bar{1}$
			0 $\bar{1}$ 0	0 1 0

pattern resulted in an R_p value of 0.060, an R_{wp} value of 0.102 and χ^2 of 9.2. The RR applied to a 2θ range from 1.0 to 30.0° ended up in a final fit between the calculated and experimental XRPD pattern with an R_p value of 0.041, an R_{wp} value of 0.055, an R_{Bragg} value of 0.081 and χ^2 of 4.4 (Fig. 4). Without correction for preferred orientation the R_p value was 0.052, the R_{wp} value 0.068, the R_{Bragg} value 0.103 and χ^2 was 5.4. The refined parameters for preferred orientation are listed in Table 2. Fig. 5 shows the packing of two β-SSS molecules in the unit cell with the c axis perpendicular to the plane of the paper.

The fractional atomic coordinates have been deposited and the value ranges of selected geometric parameters are listed in Table 5.

For correct positioning of the β-MMM and β-SSS molecules in their respective asymmetric units a relatively large amount of low-order reflections was used in the respective grid-search procedures. At low 2θ values (d-spacing values between ∼45 and ∼5.5 Å) only $hk0$ reflections are present, containing primarily information on the chain-length packing of the molecules, *i.e.* the thickness of the acyl chain layers and the tilt of the acyl chains with respect to the plane through the methyl end-groups. The high-intensity reflections originating from the lateral chain packing have d-spacing values in the range 5.26–3.63 Å. Thus, to position the molecules in their asymmetric unit successfully, it is essential to use both classes of reflections.

Like the other known members of the homologous series β-$C_nC_nC_n$-type (n = even) TAGs, both β-MMM and β-SSS were crystallized in an asymmetric tuning-fork conformation and the zigzag planes of the acyl chains are packed parallel (Figs. 3 and 5). The molecules form layers of laterally packed acyl chains bordered by either a methyl end-group plane or a glycerol moiety (Fig. 6). The structures of β-MMM and β-SSS are almost identical to each other and to the structure of β-PPP, except for a difference in chain length, as expressed by the low overall r.m.s. values (β-MMM/β-PPP 0.055, β-SSS/β-PPP 0.063 and β-MMM/β-SSS 0.066).

Figure 2
High-resolution synchrotron XRPD pattern (λ = 0.99542 Å) of β-MMM (upper), the pattern as calculated from the refined crystal structure (middle) and the difference between these patterns (lower).
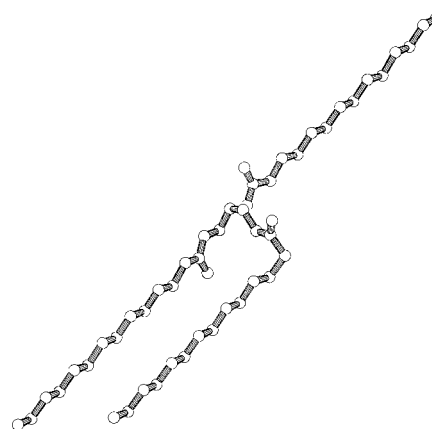

Figure 3
PLATON (Spek, 2000) representation of the β-MMM molecular conformation in the crystal structure.

van Langevelde *et al.* · β-Trimyristin and β-tristearin

Like the initially determined unit-cell parameters of β-MMM, the refined unit-cell parameters of the crystal structure of β-MMM differ little from the predicted ones (Table 1). Although these initially determined unit-cell parameters fit the unit-cell series of its structural homologues, this unit cell appeared not to be in the same unit-cell setting as the overlap model: in the structural model obtained by the grid-search procedure the acyl chains were not parallel to the b axis. Unit-cell transformation to a slightly different unit cell revealed the expected solution which does fit the overlap model (Table 1).

The refined fractional atomic coordinates of β-MMM resemble closely those predicted by Van Langevelde et al. (1999a) with the y coordinates showing the smallest differences ($|\Delta y|_{max}$ = 0.003) and the z coordinate the largest ($-0.054 \leq \Delta z \leq 0.023$). The RR module in MRIA (Zlokazov & Chernyshev, 1992) did not supply standard deviations of atomic coordinates, so a more definite conclusion concerning these differences is not possible. Moreover, the predicted atomic coordinates for β-MMM were based on predicted unit-cell parameters, but since the latter deviate slightly from the refined ones, small differences in the atomic coordinates were expected. Obviously, more accurate unit-cell parameters will lead to a better prediction of atomic coordinates. Therefore, prediction of atomic coordinates via interpolation in a structural homologous series is a valid method for determination of TAG crystal structures and should be performed with refined unit-cell parameters preferably.

The predicted unit-cell parameters for β-SSS deviate only slightly from the refined ones (Table 4) and also the unit-cell parameters determined by Skoda et al. (1967) are quite close to those determined from the high-resolution powder data. However, the unit-cell parameters for β-SSS as determined by De Jong & Van Soest (1978) show larger differences, especially the b axis and γ angle.

The crystal structures of β-MMM and β-SSS demonstrate the feasibility of structure determination of TAG series members from high-resolution X-ray powder diffraction data if a homologous single-crystal structure based overlap model is available. The small r.m.s. values of the matched structures confirm the predictive quality of this model. Obviously, the above approach is only possible as long as the TAG series exhibits linear behaviour. Small deviations from linearity of
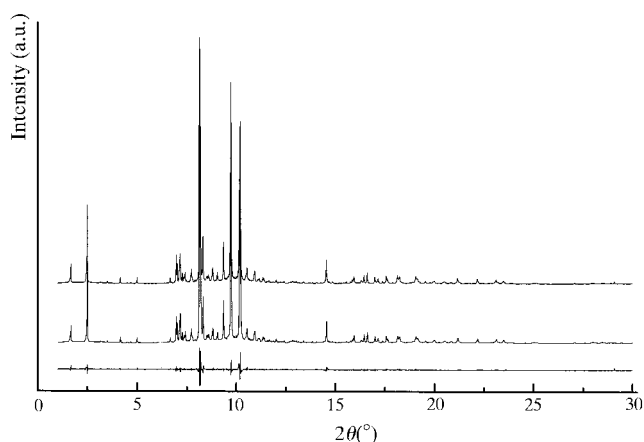

Figure 4
High-resolution synchrotron XRPD pattern [λ = 0.650515 (1) Å] of β-SSS (upper), the pattern as calculated from the refined crystal structure (middle) and the difference between these patterns (lower).
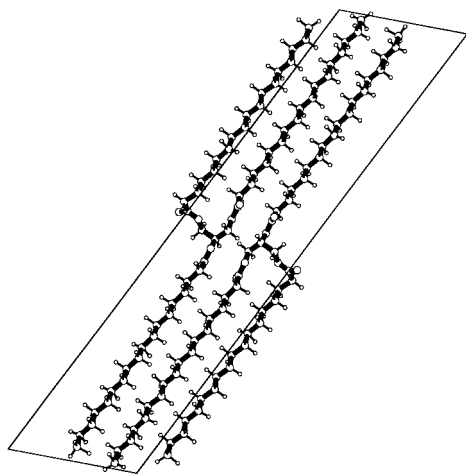

Figure 5
PLATON (Spek, 2000) representation of the two β-SSS molecules in the unit cell (c axis perpendicular to the plane of the paper), showing the parallel acyl zigzag chains.
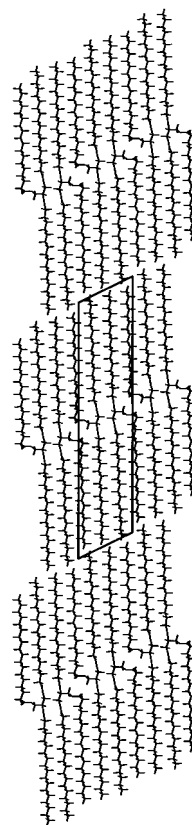

Figure 6
Crystal packing of β-SSS with the c axis perpendicular to the plane of the paper showing the parallelism of the acyl chains resulting in a layered structure.

these long-chain molecules can only be resolved by single-crystal structure determination.

References

Ahtee, M., Nurmela, M., Suortti, P. & Järvinen, M. (1989). *J. Appl. Cryst.* **22**, 261–268.
Chernyshev, V. V. & Schenk, H. (1998). *Z. Kristallogr.* **213**, 1–3.
Culot, C., Norberg, B., Evrard, G. & Durant, F. (2000). *Acta Cryst.* B**36**, 317–321.
De Jong, S. & Van Soest, T. C. (1978). *Acta Cryst.* B**34**, 1570–1583.
Doyne, T. H. & Gordon, J. T. (1968). *J. Am. Oil Chem. Soc.* **45**, 333–334.
Fitch, A. N. (1996). *Materials Science Forum*, Vol. 228, edited by R. J. Cernik, R. Delhez and E. J. Mittemeijer, pp. 219–222. Aedermannsdorf: Trans Tech Publications.
Gibon, V., Blanpain, P., Norberg, B. & Durant, F. (1984). *Bull. Soc. Chim. Belg.* **93**, 27–34.
Goto, M., Kodali, D. R., Small, D. M., Honda, K., Kozawa, K. & Uchida, T. (1992). *Proc. Natl. Acad. Sci. USA*, **89**, 8083–8086.
Holland, T. J. B. & Redfern, S. A. T. (1997). *Mineral Mag.* **61**, 65–77.
Järvinen, M. (1993). *J. Appl. Cryst.* **26**, 525–531.
Jensen, L. H. & Mabis, A. J. (1963). *Nature*, **197**, 681–682.
Jensen, L. H. & Mabis, A. J. (1966). *Acta Cryst.* **21**, 770–781.
Larsson, K. (1965). *Arkiv Kemi*, **23**, 1–15.
Molecular Simulations Inc. (1995). *Cerius*². Release 2.0. Biosym/Molecular Simulations Inc., San Diego, USA.
Rappé, A. K., Casewit, C. J., Colwell, K. S., Goddard, W. A. & Skiff, W. M. (1992). *J. Am. Chem. Soc.* **114**, 10024–10035.
Roberts, B. W. & Parrish, W. (1962). *International Tables for Crystallography*, edited by C. H. MacGillavry and G. D. Rieck, Vol. III, pp. 73–88. Birmingham: Kynoch Press. (Present distributor Kluwer Academic Publishers, Dordrecht.)
Skoda, W., Hoekstra, L. L., Van Soest, T. C., Bennema, P. & Van den Tempel, M. (1967). *Kolloid Z. Polym.* **219**, 149–156.
Spek, A. L. (2000). *PLATON*. Utrecht University, The Netherlands.
Toraya, H. (1986). *J. Appl. Cryst.* **19**, 440–447.
Van de Streek, J., Verwer, P., De Gelder, R. & Hollander, F. (1999). *J. Am. Oil Chem. Soc.* **76**, 1333–1341.
Van Langevelde, A., Van Malssen, K., Driessen, R., Goubitz, K., Hollander, F., Peschar, R., Zwart, P. & Schenk, H. (2000). *Acta Cryst.* B**56**, 1103–1111.
Van Langevelde, A., Van Malssen, K., Hollander, F., Peschar, R. & Schenk, H. (1999a). *Acta Cryst.* B**55**, 114–122.
Van Langevelde, A., Van Malssen, K., Sonneveld, E., Peschar, R. & Schenk, H. (1999b). *J. Am. Oil Chem. Soc.* **76**, 603–609.
Visser, J. W. (1969). *J. Appl. Cryst.* **2**, 89–95.
Zlokazov, V. B. & Chernyshev, V. V. (1992). *J. Appl. Cryst.* **25**, 447–451.